Supplementary Information

Highly Adhesive, Fluorine-Free Binders Enabled by Chemical Anchoring for Durable High-Nickel Cathodes in Lithium-Ion Batteries

Seunghyeon Kim,[1] Yeong Hun Jeong,[1] Gwangbin Won,[1] Min Seo Jo,[1] Daun Jeong,[2,] Jimin Shim[1,*]

[1]Department of Chemistry Education, Seoul National University, Seoul 08826, Republic of Korea, [2]Department of Chemical Engineering and Materials Science, University of Minnesota, Minneapolis, Minnesota 55455, United States

* E-mail: jiminshim@snu.ac.kr (J. Shim)

Table S1. Comparison of peel strength, active material loading, and electrochemical cycling performance of fluorine-free binders.

Binders	Peel strength (gf mm^{-1})	Active material loading (mg cm^{-2})	C-rate	Capacity retention[a]	Ref.
PNB	124.56	10	0.5 C	82%@300 cycles	This work
PI(BBP)	55.54	9	0.2 C	88%@100 cycles	R1[1]
LTPI	32.94	5-6	0.2 C	84.9%@100 cycles	R2[2]
PEMS	-	-	0.5 C	80.6%@200 cycles	R3[3]
SPIO	39.77	6	0.5 C	80%@300 cycles	R4[4]
PI-OmDT	52.31	5	0.5 C	91.6%@100 cycles	R5[5]
CMC	–	2	0.1 C	96.4%@100 cycles	R6[6]
PAA-PN	–	2.5-2.8	0.5 C	91.7%@400cycles	R7[7]

[a]All cells were cycled with NCM811||Li configuration at an upper-cutoff voltage of 4.3 V.

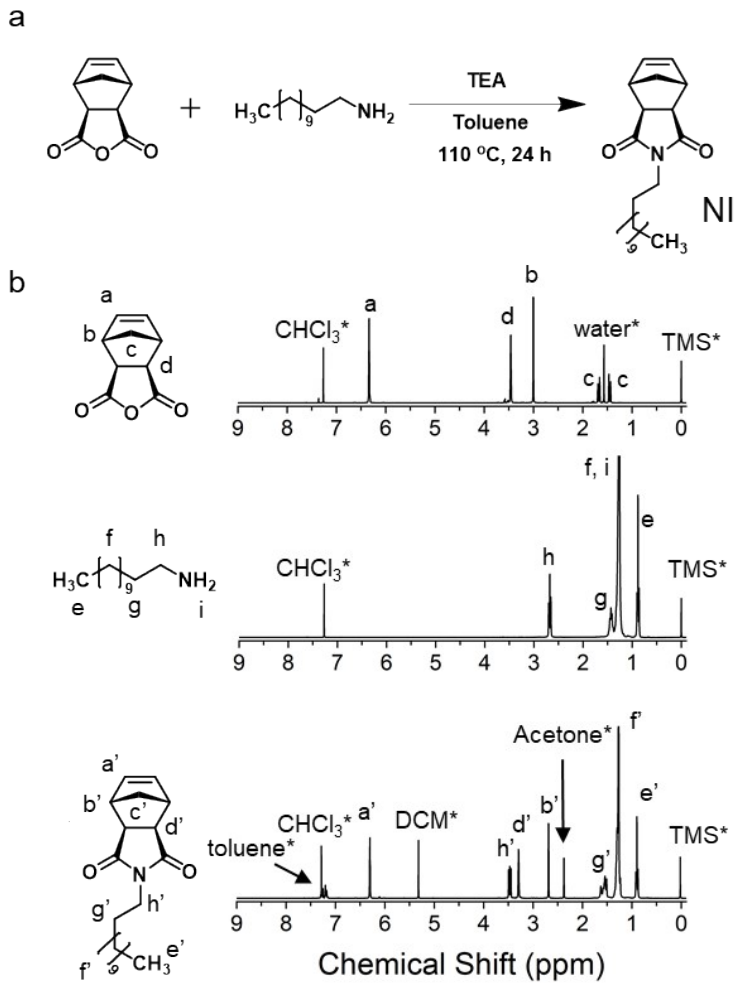

Fig. S1. a) Synthetic route to NI. b) ^{1}H NMR spectra of the reagents and the product.

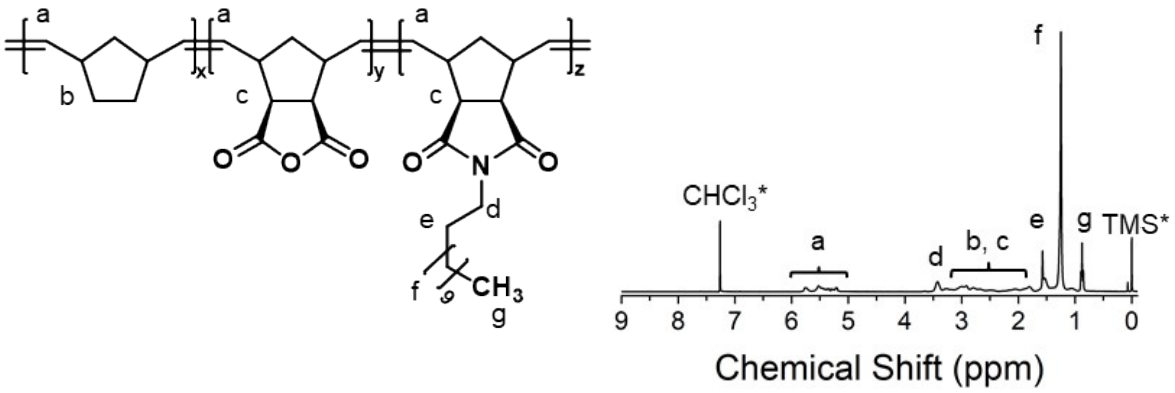

Fig. S2. ^{1}H NMR spectrum of PNB.

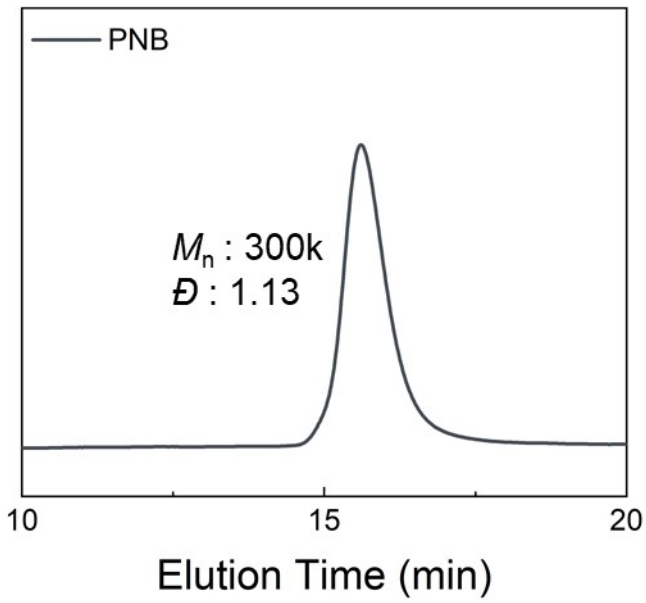

Fig. S3. SEC chromatogram of PNB.

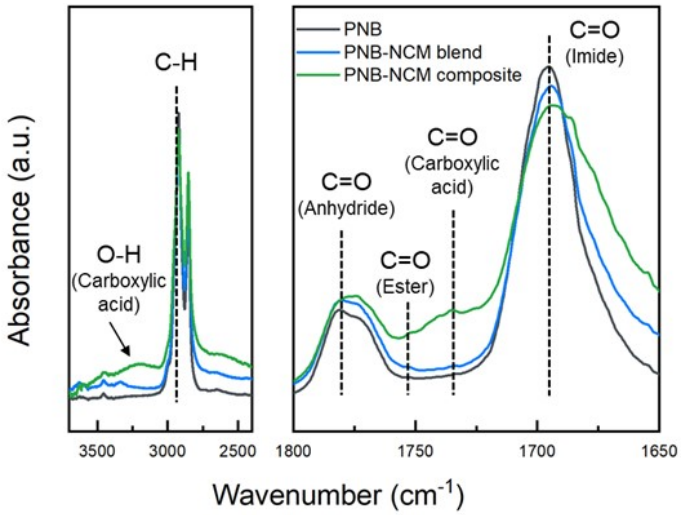

Fig. S4. FT-IR spectra of PNB, PNB-NCM blend (without thermal treatment), and PNB-NCM composite (after electrode drying at 120 °C).

No significant spectral changes are observed upon simple physical mixing, whereas the thermally treated composite exhibits the disappearance of anhydride C=O bands and the emergence of ester-related peaks, indicating covalent bond formation via a thermally activated ring-opening reaction at the NCM surface.

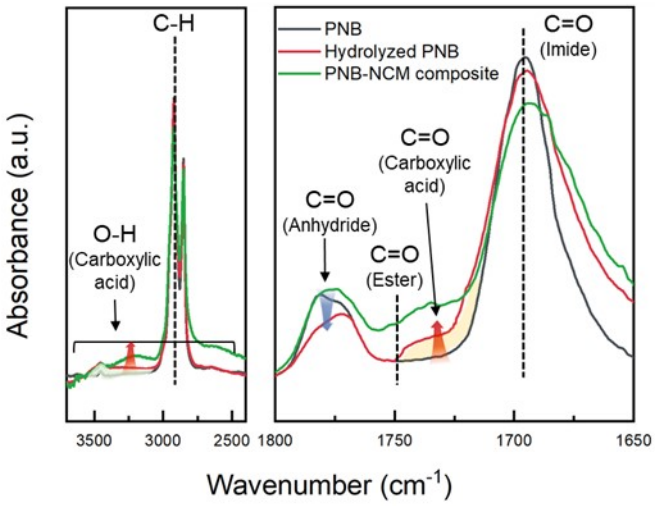

Fig. S5. FT-IR spectra of the pristine PNB and intentionally hydrolyzed PNB.

To exclude a possibility that the spectroscopic changes may result from bulk polymer transformation or side reactions, such as hydrolysis of anhydride moieties, rather than from chemical anchoring at the NCM interface, FT-IR spectra of pristine PNB and intentionally hydrolyzed PNB were compared. In the hydrolyzed PNB sample, a clear decrease in the anhydride C=O peak is observed, accompanied by a pronounced increase in the signal corresponding to carboxylic acid groups, confirming the conversion of anhydride functionalities through hydrolysis. Notably, no ester-related peaks are detected in this control sample. In contrast, the PNB–NCM composite exhibits both carboxylic acid signals and a distinct ester peak, indicating that ester formation does not originate from bulk hydrolysis but arises specifically from an interfacial reaction between PNB and the NCM surface.

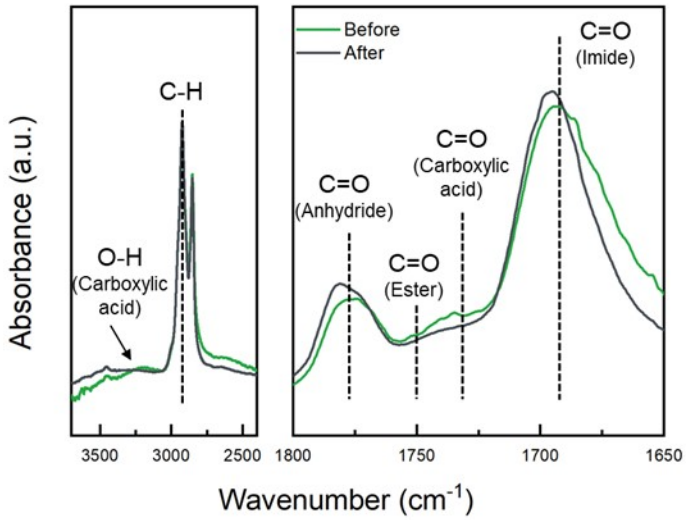

Fig. S6. FT-IR spectra of the pristine PNB-NCM composite before and after immersion in NMP for 24 h.

If the observed spectral changes originated from bulk polymer transformation or soluble byproducts, these species would be expected to dissolve during solvent treatment and thus not be retained in the solid phase. However, the FT-IR spectra recorded before and after NMP soaking remain nearly identical, with all key functional group signals clearly preserved. This result indicates that the ester functionalities are not formed as soluble byproducts but are strongly immobilized within the composite, consistent with their formation via covalent bonding at the NCM surface. These findings further support the proposed chemical anchoring mechanism and its resistance to solvent-induced leaching.

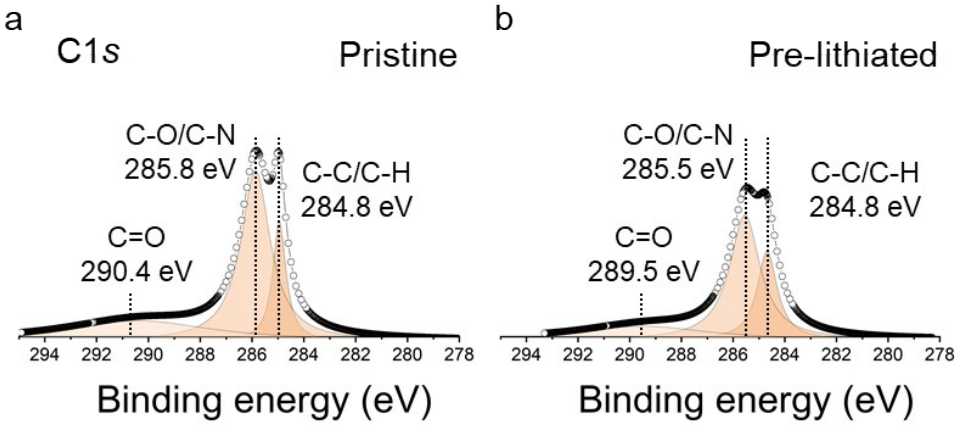

Fig. S7. XPS spectra (C1*s*) of a) pristine and b) pre-lithiated PNB cathodes.

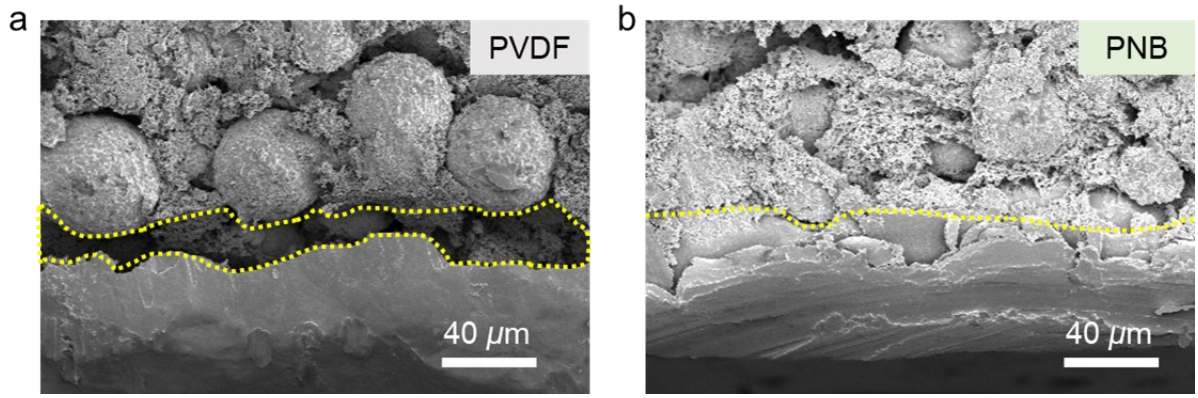

Fig. S8. Cross-sectional SEM images of a) PVDF and b) PNB cathodes.

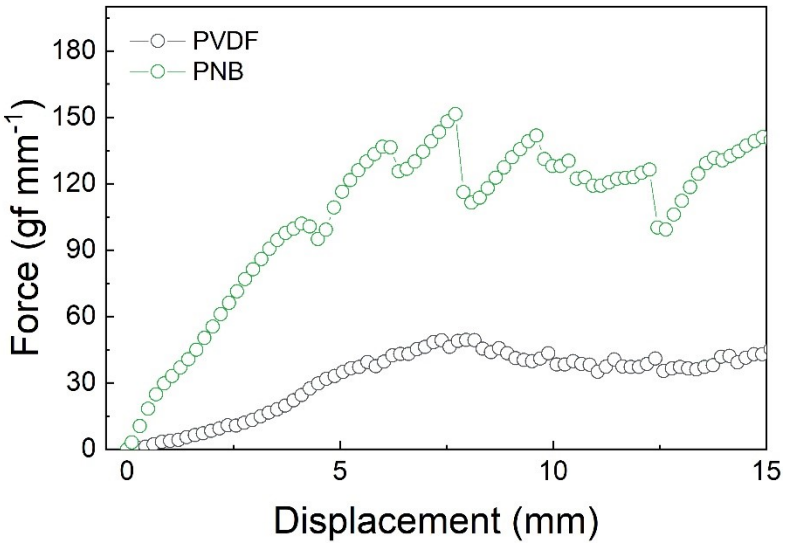

Fig. S9. 180° peel test profiles of PVDF and PNB cathodes.

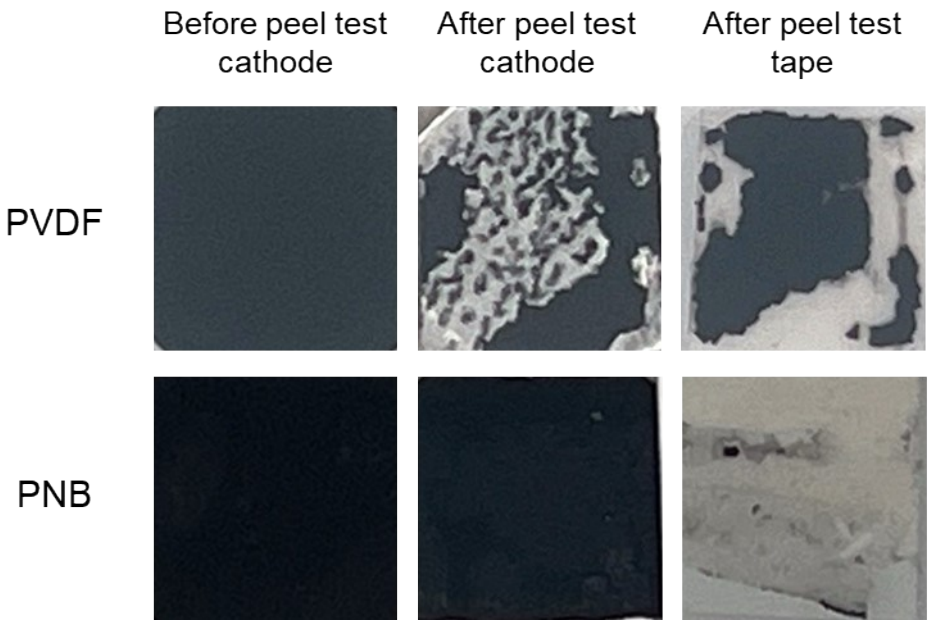

Fig. S10. Optical photographs of the cathodes and adhesive tapes used in the peel test.

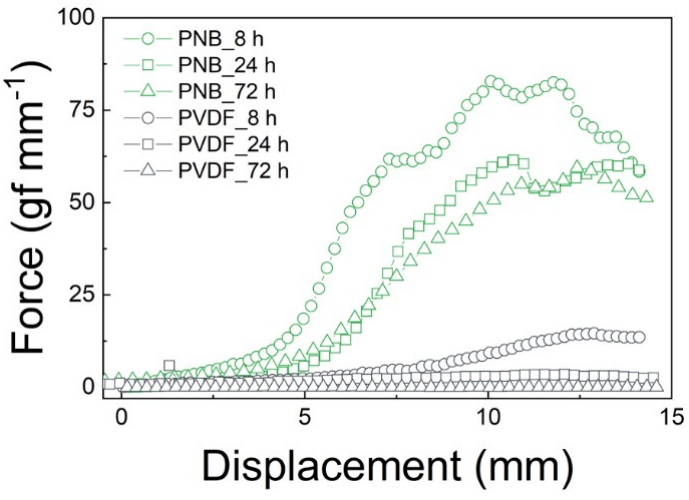

Fig. S11. 180° peel test profiles of PVDF and PNB cathodes immersed in electrolytes for different duration.

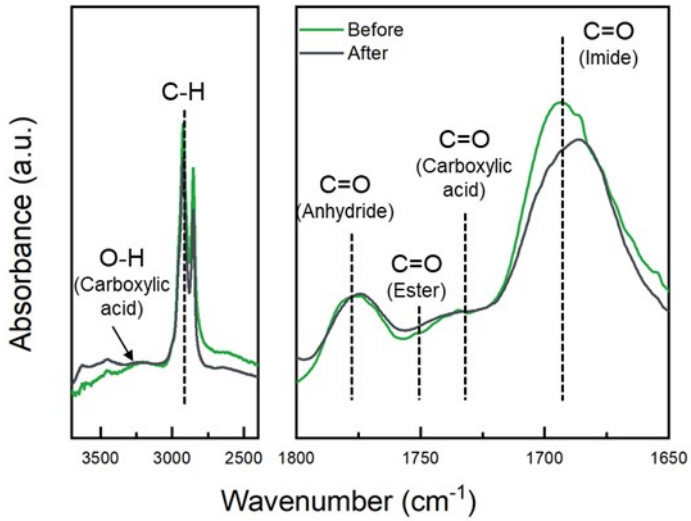

Fig. S12. FT-IR spectra of the pristine PNB-NCM composite before and after immersion in electrolyte for 24 h.

The key functional group signals, including the ester C=O band (1735–1750 cm^{-1}), remain essentially unchanged after electrolyte exposure. The absence of spectral changes associated with hydrolysis (ester loss or increased –OH/COOH signals) indicates that the interfacial covalent linkages are stable under electrolyte conditions.

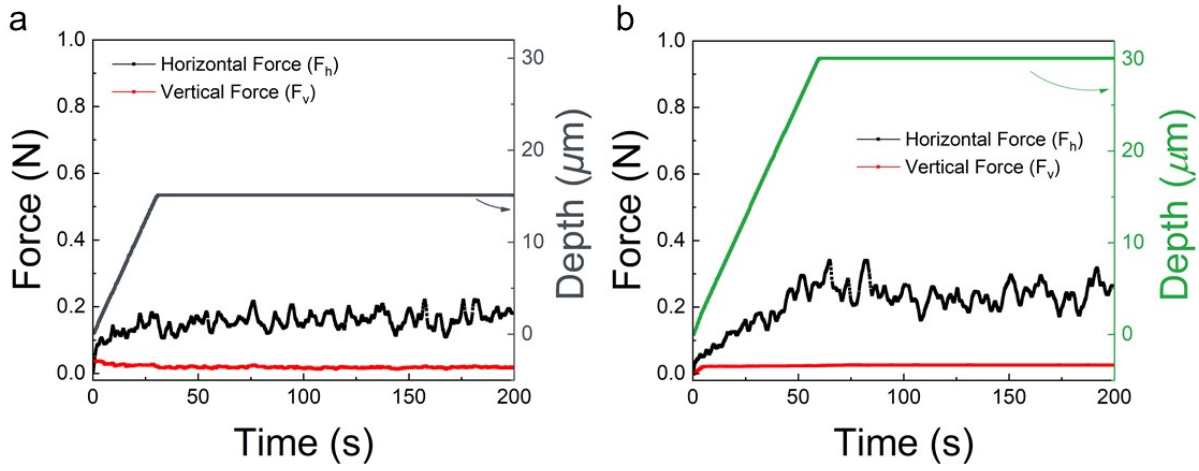

Fig. S13. SAICAS profiles of the NCM cathodes prepared with a) PVDF and b) PNB. A blade was inserted with a rake and clearance angles of 20° and 10°, respectively.

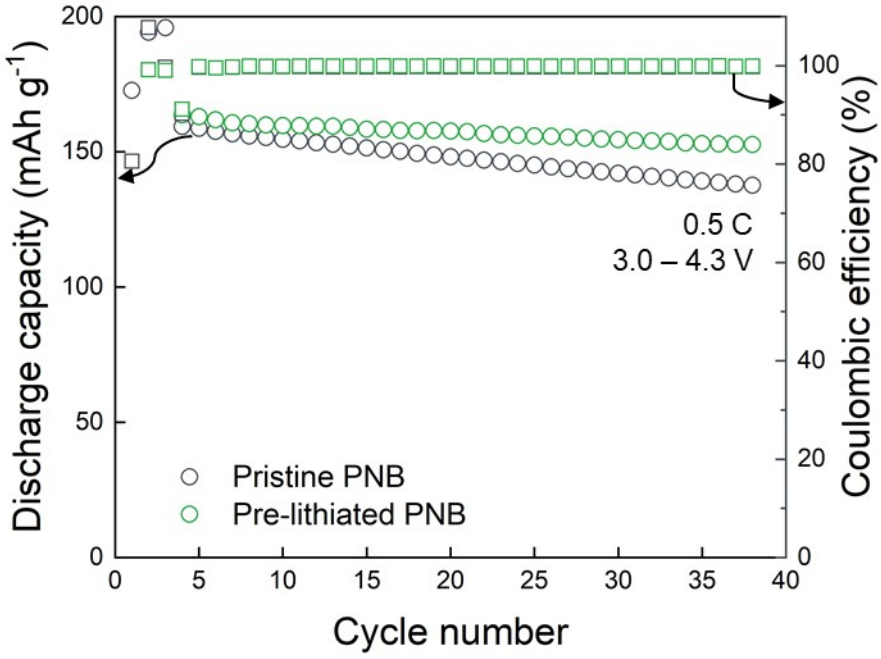

Fig. S14. Cycling performance of pristine PNB and pre-lithiated PNB cathodes.

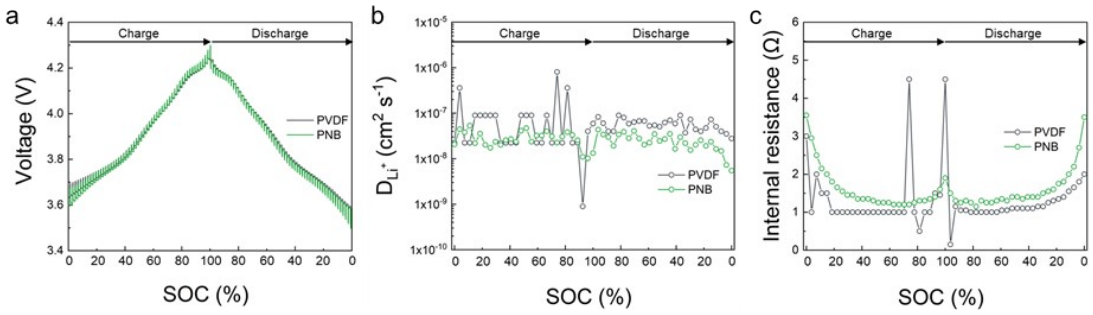

Fig. S15. a) Galvanostatic intermittent titration technique (GITT) profiles for the PVDF and PNB cathodes in a voltage range of 3.0–4.3 V. b) Evolution of Li^+ diffusion coefficient (D_{Li^+}) as a function of state-of-charge (SOC) determined by GITT. c) Evolution of internal resistance as a function of SOC determined by GITT.

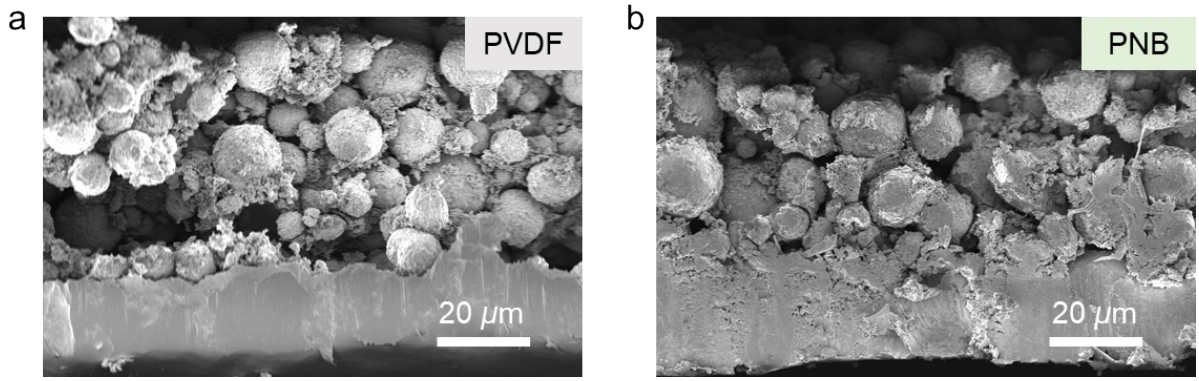

Fig. S16. Cross-sectional SEM images of a) PVDF and b) PNB cathodes with lean binder condition (2 wt%).

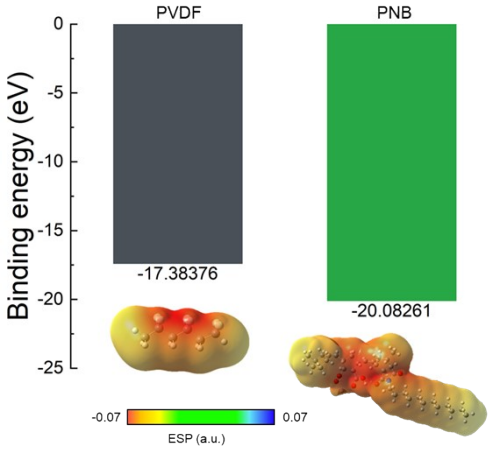

Fig. S17. Calculated binding energies of PVDF and PNB with Ni^{2+} and their electrostatic potential maps.

References for Supporting Information

1 K. Qi, Y. Wang, N. Dong, B. Liu, G. Tian, S. Qi, D. Wu, *Appl. Energy*, 2022, **320**, 119282.
2 C. Wang, Y. Kang, B. Liu, D. Lin, G. Tian, S. Qi, D. Wu, *ACS Sustainable Chem. Eng.*, 2025, **13**, 7687–7697.
3 Y. Xu, F. Z. Chafi, P. Chen, C. Peng, Y.-J. Cheng, K. Guo, X. Zuo, Y. Xia, *ACS Appl. Polym. Mater.*, 2023, **5**, 4654–4663.
4 H. Peng, L. Liu, Q. Zhang, S. Liu, M. Lin, H. Li, Y. Deng, C. Jiao, C. Wang, H. Xu, *Chin. J. Polym. Sci.*, 2025, **43**, 1146–1154.
5 Y. Xu, Y. Wang, N. Dong, C. Pu, B. Liu, G. Tian, S. Qi, D. Wu, *J. Energy Chem.*, 2023, **76**, 19–31.
6 Z.Chen, G-. T. Kim, D. Chao, N. Loeffler, M. Copley, J. Lin, Z. Shen, S. Passerini, *J. Power Sources*, 2017, **372**, 180–187.
7 H. Wang, F. Zhang, N. Qin, Z. Wang, Y. Wang, Z. Wang, C. Zeng, H. Li, Q. Liu, Y. Li, Z. Lu, D. Luo, H. Cheng, *ACS Energy Lett.*, 2025, **10**, 136–144.